CHINESE PHYSICAL SOCIETY | IOP Publishing
CPB
Chinese Physics B
http://cpb.iphy.ac.cn https://iopscience.iop.org/journal/1674-1056

Quantitative simulations of ratchet potential in a dusty plasma ratchet

Shuo Wang(王硕), Ning Zhang(张宁), Shun-Xin Zhang(张顺欣), Miao Tian(田淼), Ya-Wen Cai(蔡雅文), Wei-Li Fan(范伟丽), Fu-Cheng Liu(刘富成), and Ya-Feng He(贺亚峰)

Citation: Chin. Phys. B, 2022, 31 (**6**): 065202. DOI: 10.1088/1674-1056/ac46c4
Journal homepage: http://cpb.iphy.ac.cn; http://iopscience.iop.org/cpb

Quantitative simulations of ratchet potential in a dusty plasma ratchet

Shuo Wang(王硕), Ning Zhang(张宁), Shun-Xin Zhang(张顺欣), Miao Tian(田淼),
Ya-Wen Cai(蔡雅文), Wei-Li Fan(范伟丽), Fu-Cheng Liu(刘富成)†, and Ya-Feng He(贺亚峰)‡

College of Physics Science and Technology, Institute for Life Sciences and Green Development, Hebei University, Baoding 071002, *China*

(Received 23 November 2021; revised manuscript received 28 December 2021; accepted manuscript online 29 December 2021)

Using a dusty plasma ratchet, one can realize the rectification of charged dust particle in a plasma. To obtain the ratchet potential dominating the rectification, here we perform quantitative simulations based on a two-dimensional fluid model of capacitively coupled plasma. Plasma parameters are firstly calculated in two typical cross sections of the dusty plasma ratchet which cut vertically the saw channel at different azimuthal positions. The balance positions of charged dust particle in the two cross sections then can be found exactly. The electric potentials at the two balance positions have different values. Using interpolation in term of a double-sine function from previous experimental measurement, an asymmetrical ratchet potential along the saw channel is finally obtained. The asymmetrical orientation of the ratchet potential depends on discharge conditions. Quantitative simulations further reproduce our previous experimental phenomena such as the rectification of dust particle in the dusty plasma ratchet.

Keywords: dusty plasma, ratchet potential

PACS: 52.27.Lw, 52.27.Gr, 52.65.Kj **DOI:** 10.1088/1674-1056/ac46c4

1. Introduction

Brownian ratchets refer to a structure consisting of periodical and asymmetrical units in one or two dimensions.[1–9] It can rectify the random Brownian motion of particles to generate a directed steady-state flow of particles, and has attracted great interests from diverse areas of science and technology, such as the Hamiltonian quantum ratchet,[5–7] the optical rocking ratchet,[8] and the organic electronic ratchet.[9] The ratchet potential of Brownian ratchet breaks spatial symmetry due to the asymmetrical structure. Driven by nonequilibrium perturbations such as zero-mean external biases, Brownian particles can be rectified into directional movement. The particles could be either without interaction, such as the colloidal spheres in a silicon membrane,[10] or with interaction among them, such as the electron in organic electronic ratchets.[9] Complex interaction among the charged particles gives rise to many novel phenomena such as the reversal of particle flow.

Recently, we experimentally observed the rectification of charged dust particles in a dusty plasma ratchet.[11,12] The dust particles can directionally flow in positive or negative direction along the saw channel just by changing simply the gas pressure. In this process, a ratchet potential could appear to dominant the directional transport of dust particle. The asymmetrical orientation of the ratchet potential should depend on the discharge condition. Here, we perform quantitative simulations to find this ratchet potential along the saw channel in detail. Numerical simulations show that the potential at the balance position of dust particle exhibits ratchet-like distribution along the saw channel. Using molecular dynamics simulations, we reproduce the experimental observations that dust particles can flow in opposite directions at different gas pressures.

2. Experimental setup

In order to obtain the ratchet potential we design a model of dusty plasma ratchet in which two gears are placed concentrically on the horizontal lower electrode as shown in Fig. 1. The two gears have the same asymmetrical orientation and sawtooth number, and enclose a saw channel between them. The width of the saw channel changes periodically and asymmetrically along the saw channel. Here, we choose two typical cross sections cutting vertically the saw channel in r–z plane just at different azimuthal positions, which are the widest one $\Omega_{\rm w}$ at $\theta_{\rm w}$ and the narrowest one $\Omega_{\rm n}$ at $\theta_{\rm n}$. Within each sawtooth, due to the periodicity and the asymmetry, $\Delta\theta_{\rm w}+\Delta\theta_{\rm n}=\Theta$, $\Delta\theta_{\rm w}/\Delta\theta_{\rm n}=2/13$, here $\Theta=2\pi/24$ is the period of the gears. One of the typical cross sections is shown by the color section in Fig. 1. This dusty plasma ratchet is placed in a vacuum chamber filled with argon gas and plasma is generated by capacitive coupling discharge (13.56 MHz). The dust particles used are monodisperse polystyrene microspheres with a radius of 11.5 μm. The rectification and reversal of the dust particles in the plasma ratchet is accomplished by changing the pressure and the discharge power.

The 3D distributions of plasma parameters $\Pi(r,z,\theta)$ are actually hard to calculate directly at present. Here, we adopt

†Corresponding author. E-mail: hdlfc@hbu.edu.cn
‡Corresponding author. E-mail: heyf@hbu.edu.cn

 http://iopscience.iop.org/cpb http://cpb.iphy.ac.cn

two steps to resolve this issue as shown below. Firstly, we perform COMSOL[13] simulations in the r–z plane to obtain the plasma parameters $\Pi(r,z)$ in the two typical cross sections $\Omega_{\rm w}$ and $\Omega_{\rm n}$. Secondly, the plasma parameters in other cross sections besides the two typical cross sections can be interpolated in term of a double-sine function because the dependance of plasma parameters on θ can be fitted well by the double-sine function.[11]

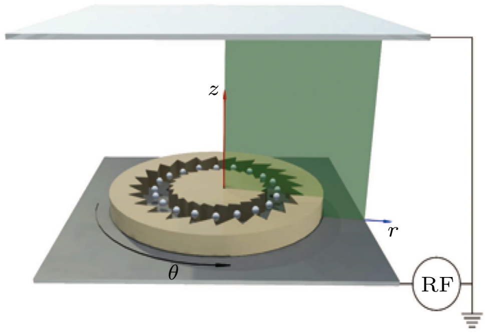

Fig. 1. Diagram of the dusty plasma ratchet. Two gears with asymmetrical sawtooth are placed concentrically on the lower electrode and enclose a saw channel in which dust particles flow persistently in θ-direction. The gray region illustrates one of the two typical cross sections $\Omega_{\rm n,w}$ cutting vertically the saw channel in r–z space, in which numerical simulations are performed.

3. Experimental results

Figure 2 shows the distributions of electron density $n_e(r,z)$ and electric potential $U(r,z)$ in r–z plane in the widest cross section. It can be seen that the plasma can deepen into the saw channel and the equipotential curves near the saw channel exhibit parabolic-like distribution which can confine charged dust particle to the center of the saw channel. Based on the calculated plasma parameters the charge Q of dust particle can be obtained using the orbital-motion-limited theory, $Q \sim 10^4 e$. Then, the acting force on dust particle in the two typical cross sections can be analyzed as shown below.

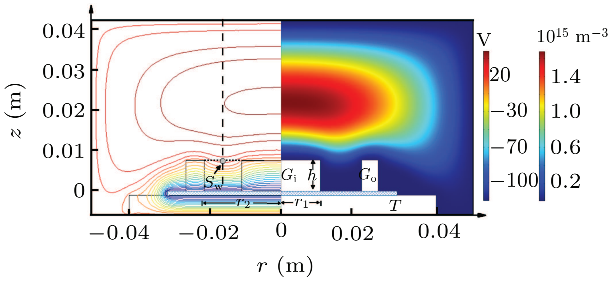

Fig. 2. Distributions of electron density (right) and potential (left) in cross section $\Omega_{\rm w}$ in r–z plane. $G_{\rm i}$, $G_{\rm o}$, and T represent the cross sections of the inner and outer gears, and the teflon block, respectively; $r_1 = 11$ mm, $r_2 = 21$ mm, and $h = 9$ mm. Grey stripe indicates the powered electrode. Spot $S_{\rm w}$ indicates the balance position of dust particle in the saw channel. Boundaries of the chamber are grounded. Gas pressure 40 Pa and rf power 10 W ($V_0 = 39$ V, $V_{\rm dc} = -112$ V).

We consider the acting force on dust particle in the r and z directions, respectively. In the radial r-direction, because the equipotential curves of different values all exhibit parabolic distribution as shown in Fig. 2, the charged dust particle will be definitely confined to the center of the saw channel although the dust particle could be levitated at different heights. Figure 3 shows the balance positions of dust particle in the radial and vertical directions, respectively, in which the dashed lines S_r indicate the balance positions of dust particle at different heights. It shows that, in both the widest and narrowest cross sections, dust particle is confined to the center of the saw channel $r_{\rm c} \approx 15.1$ mm.

In the vertical direction, the gravity of dust particle is balanced by the electric field in the sheath of the lower electrode. The balance height of dust particle at different radii of the saw channel is indicated by the solid curves S_z in Fig. 3. Obviously, from the individual balance position in the radial and vertical directions, the intersection of the solid curve S_z and the dashed line S_r is the actual balance position of dust particle in the saw channel. It can be seen that the balance height $S_{\rm n}$ of dust particle in the narrowest cross section is always higher than that $S_{\rm w}$ in the widest cross section even if the discharge condition is different. The difference Δz between the two balance heights $S_{\rm n}$ and $S_{\rm w}$ is in the range from about several tens to a few hundreds of µm, depending on discharge conditions. It is clear that, besides the two typical cross sections, the balance heights in other cross sections would be located between the two points, i.e., the maximum $S_{\rm n}$ and the minimum $S_{\rm w}$.

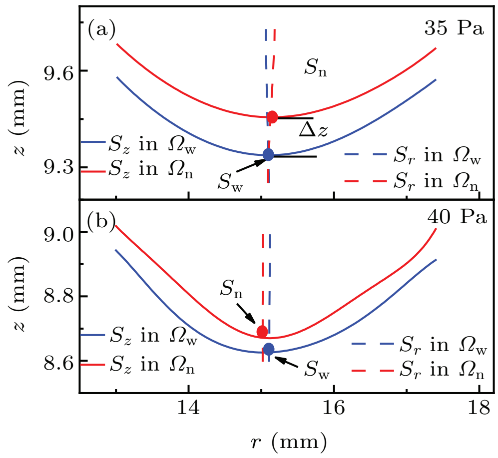

Fig. 3. Balance positions $S_{\rm n}$ and $S_{\rm w}$ of the charged dust particle in the two typical cross sections $\Omega_{\rm n}$ and $\Omega_{\rm w}$, respectively. Solid curves represent the balance height of dust particle in z-direction above the lower electrode at different radii. Dashed lines indicate the balance position in r-direction at different heights. Thus, the intersections of $S_{\rm n}$ and $S_{\rm w}$ of the solid curves and the dashed lines are the actual balance positions of the dust particle in the vertical section. Notably, $S_{\rm n}$ in the narrowest cross section $\Omega_{\rm n}$ is always higher than $S_{\rm w}$ in the widest cross section $\Omega_{\rm w}$. The higher the gas pressure is, the lower the balance position is. The radius of the dust particle is $r_{\rm d} = 11.5$ µm.

We next focus on the potential at the balance position of the dust particle. Figure 4 shows the distribution of potential along the vertical dashed line passing the balance position $S_{\rm n,w}$ in Fig. 2. It can be seen that the potential drops dramatically across the sheath of the lower electrode. From the calculated balance height $S_{\mathrm{n,w}}$ in Fig. 3, we mark the balance position $S_{\mathrm{n,w}}$ of dust particle as colored spots as indicated in the enlarged view in Fig. 4, and then can find the potential at the balance height. It can be seen that the balance height of dust particle at higher gas pressure $p = 40$ Pa is lower than that at lower gas pressure $p = 35$ Pa, and the balance height S_{n} in the narrowest cross section Ω_{n} is always higher than that S_{w} in the widest cross section Ω_{w} for the two gas pressures. However, we find that the potential U_{n} at S_{n} is smaller than that U_{w} at S_{w} at $p = 40$ Pa, whereas U_{n} at S_{n} is larger than that U_{w} at S_{w} at $p = 35$ Pa, which results in the reversal of asymmetrical orientation of ratchet potential at the two gas pressures as shown later.

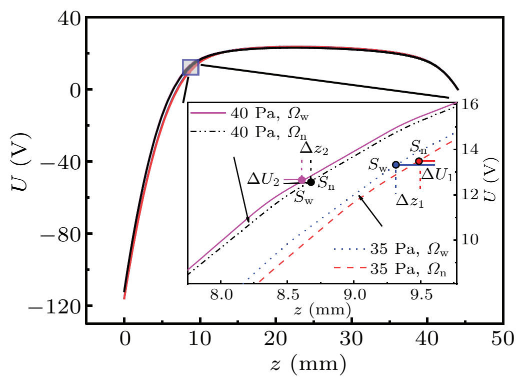

Fig. 4. Electric potential in the vertical dashed line in Fig. 2. Solid spots in the enlarged view indicate the balance positions S_{n} and S_{w}, where the potentials are somewhat different so as to give rise to a ratchet potential along the saw channel. $U_{\mathrm{n}} > U_{\mathrm{w}}$ at 35 Pa, whereas $U_{\mathrm{n}} < U_{\mathrm{w}}$ at 40 Pa, which illustrates that the asymmetrical orientation of the ratchet potential reverses at the two gas pressures. Parameters are the same as those in Fig. 3.

Our previous work proved that, along the saw channel, the distributions of dust particles and plasma parameters have the ratchet-like character, which is attributed to the asymmetry of sawtooth.[11] The dependance of plasma parameters on θ can be depicted by an asymmetrical double-sine function

$$\Pi(\theta) = A\left(\sin\left(2\pi\frac{\theta}{\Theta}\right) + \frac{1}{4}\sin\left(4\pi\frac{\theta}{\Theta}\right)\right) + B, \tag{1}$$

where Θ is the period of the sawtooth. We interpolate the potential of balance height along the saw channel using this double-sine function that passes the balance position S_{n} and S_{w},

$$U(\theta) = U_0\left(\sin\left(2\pi\frac{\theta}{\Theta}\right) + \frac{1}{4}\sin\left(4\pi\frac{\theta}{\Theta}\right)\right) + U_1. \tag{2}$$

Here, U_0 and U_1 are the amplitude and the bias of the electric ratchet potential,

$$U_0 = (U_{\mathrm{n}} - U_{\mathrm{w}})/2, \tag{3}$$

$$U_1 = (U_{\mathrm{n}} + U_{\mathrm{w}})/2. \tag{4}$$

Figure 5 shows the calculated ratchet potential along the saw channel at two gas pressures. Due to the asymmetry of the sawtooth the ratchet potential exhibits the character of asymmetry. From the quantitative results in Figs. 3 and 4, for the case $p = 35$ Pa, the potential U_{n} at S_{n} is higher than U_{w} at S_{w}, which gives rise to the left orientation of the ratchet potential. However, for the case $p = 40$ Pa, the potential U_{n} at S_{n} is lower than U_{w} at S_{w}, which gives rise to the right orientation of the ratchet potential. As shown in Ref. [11], the asymmetrical ratchet potential gives rise to an azimuthal electric field, which further results in an ion drag $F_{\mathrm{i}\theta}$ pushing the dust particle. We define a net ion drag force as $f_{\mathrm{i}\theta}(r) = \frac{\oint_{l(r)} \boldsymbol{F}_{\mathrm{i}\theta}(r)\cdot \mathrm{d}\boldsymbol{l}(r)}{l(r)}$, a circulation of $F_{\mathrm{i}\theta}$ divided by the circular path of integration $l(r)$. Figure 6 shows the net force of ion drag $f_{\mathrm{i}\theta}$ at 35 Pa and 40 Pa along the horizontal dotted line within the saw channel in Fig. 2. It can be seen that the peak of the net force of ion drag appears near the center $r \approx 15.1$ mm of the saw channel, and this net force is of order of 10^{-13} N, which can overcome the dissipation neutral drag $\sim 10^{-13}$ N to drive the dust chain to flow along the saw channel. However, the signs of the net force of ion drag for the two gas pressures are opposite. Figures 5 and 6 show clearly that the asymmetrical orientation of the ratchet potential can reverse at different gas pressures, which definitely results in the opposite signs of the net ion drag and the opposite flow of dust chain along the saw channel. Noticeably, in the above simulation with a particle radius of $r_{\mathrm{d}} = 11.5$ μm, the potential of the balance height determines the asymmetrical orientation of the ratchet potential. We also test our conclusions both numerically and experimentally with different particle radii (not shown here). We find that, although the balance heights of different sizes particle are different, the qualitative conclusions still hold, which means that different sizes particles can be rectified just by changing discharge conditions in the dusty plasma ratchet.

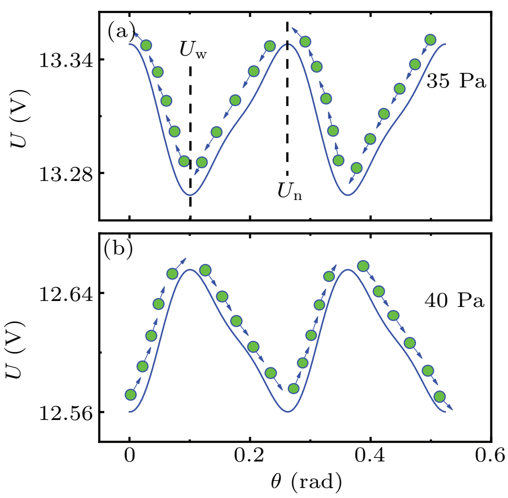

Fig. 5. Electric potential in the balance position of dust particle within two sawteeth along the saw channel. The electric potentials distribute asymmetrically and the orientation of this ratchet potential at 35 Pa is opposite to that at 40 Pa. Green solid spots represent the dust chain flowing in the arrow direction. U_{n} and U_{w} are the potentials at balance heights in Fig. 4.

In our simulations, we obtain the ratchet potential along the saw channel by interpolating the numerical calculation in two typical cross sections. In order to verify the validity of the interpolation, we also perform simulation in other cross section between the two typical cross sections. We find that the balance height of dust particle in this test cross section is located between $S_{\rm n}$ and $S_{\rm w}$, and the potential at this balance height is also located between $U_{\rm n}$ and $U_{\rm w}$. Our tested results clearly show that these interpolation results are the same for the simulation results.

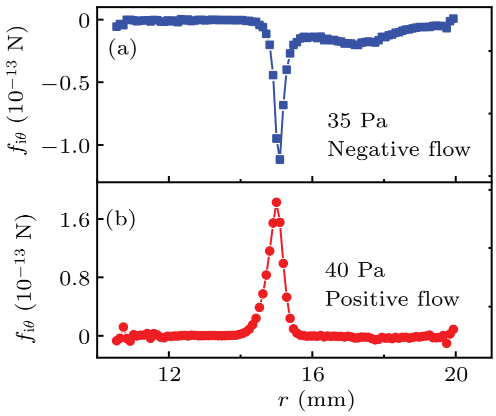

Fig. 6. Radial distribution of the net ion drag force, with $f_{i\theta}(r) < 0$ ($f_{i\theta}(r) > 0$) leading to the negative (positive) flow of the dust particles. The peaks of curves appear around the center of the saw channel at $r \approx 15.1$ mm, where the dust particles distributed. Parameters are the same as those in Fig. 5.

4. Conclusion

In summary, we have quantitatively study the asymmetrical ratchet potential along the saw channel of the dusty plasma ratchet. Using numerical simulations, we firstly obtain the plasma parameters in two typical cross sections cutting vertically the saw channel, and find out the balance positions of charged dust particle in the two cross sections. The potentials at the two balance positions are somewhat different. Then, in the azimuthal direction along the saw channel, we deduce a ratchet potential of balance position of dust particle through interpolation with a double-sine function. We further find that the asymmetrical orientations of the ratchet potential and the signs of the net force of ion drag for different gas pressures are opposite. Numerical results explain quantitatively the reversal of dust flow in the dusty plasma ratchet under different discharge conditions.

Acknowledgements

Project supported by the National Natural Science Foundation of China (Grant Nos. 11975089 and 11875014), the Interdisciplinary Research Program of Natural Science of Hebei University (Grant No. DXK202010), and the Hebei Natural Science Fund (Grant Nos. A2021201003 and A2021201010).

References

[1] Feynman R P, Leighton R B and Sands M 1963 *The Feynman Lectures on Physics* (Reading, MA: Addison-Wesley) Vol. I
[2] Hänggi P and Marchesoni F 2009 *Rev. Mod. Phys.* **81** 387
[3] Reimann P 2002 *Phys. Rep.* **361** 57
[4] Drexler C, Tarasenko S A, Olbrich P *et al*. 2013 *Nat. Nanotech.* **8** 104
[5] Salger T, Kling S, Hecking T *et al*. 2009 *Science* **326** 1241
[6] Grossert C, Leder M, Denisov S *et al*. 2016 *Nat. Commun.* **7** 10440
[7] Silva C C de S, Van de Vondel J, Morelle M *et al*. 2006 *Nature* **440** 651
[8] Arzola A V, Volke-Sepúlveda K and Mateos J L 2011 *Phys. Rev. Lett.* **106** 168104
[9] Roeling E M, Germs W C, Smalbrugge B *et al*. 2011 *Nat. Mater.* **10** 51
[10] Matthias S and Müller F 2003 *Nature* **424** 53
[11] He Y F, Ai B Q, Dai C X *et al*. 2020 *Phys. Rev. Lett.* **124** 075001
[12] Dai C X, Song C, Zhou Z X *et al*. 2020 *Chin. Phys. B* **29** 025203
[13] *COMSOL Multiphysics* version 5.3a, www.comsol.com